

Synthesis of Conjugated Tetrathiafulvalene (TTF)- π -Acceptor Molecules – Intramolecular Charge Transfer and Nonlinear Optical Properties

Martin R. Bryce,^{*,[a]} Andrew Green,^[a] Adrian J. Moore,^[a] Dmitrii F. Perepichka,^[a] Andrei S. Batsanov,^[a] Judith A.K. Howard,^[a] Isabelle Ledoux-Rak,^[b] Mar González,^[c] Nazario Martín,^{*,[c]} José L. Segura,^[c] Javier Garín,^[d] Jesús Orduna,^[d] Rafael Alcalá,^[e] and Belén Villacampa^[e]

Keywords: Ab initio methods / Charge-transfer / Crystal structure / Nonlinear optics / Tetrathiafulvalene

We have synthesised new conjugated donor- π -acceptor (D- π -A) chromophores **7**, **9**, and **12–15** in which monosubstituted tetrathiafulvalene (TTF) and trimethyl-TTF units are the donor moieties, connected by ethylenic bridges to electron-deficient benzene derivatives as the acceptor moieties. These compounds display a broad intramolecular charge transfer (ICT) band in their solution UV/Vis spectra at λ_{max} = ca.

500 nm. The second order nonlinear optical (NLO) properties of these derivatives have been studied using the EFISH technique and calculated by semiempirical and ab initio theoretical methods. The effect of methyl substituents in the TTF moiety and the nature of the conjugated bridge are discussed. Analysis of the bond lengths obtained by an X-ray diffraction study of compound **9** reveal ICT in the solid state.

Introduction

Organic molecules which contain electron donor (D) and electron acceptor (A) units linked by a π -conjugated bridging group (D- π -A systems) are currently of interest as second order nonlinear optical (NLO) materials, the study of which is important for the development of high performance electrooptic switching elements for telecommunications and optical information processing.^[1] It has become apparent that in this field organic materials offer many advantages over traditional inorganic crystals, such as lithium niobate, as the organics are cheaper to produce, easier to fabricate and compatible with existing semiconductor technology. Moreover, the versatility of organic synthesis should enable NLO properties to be fine-tuned for desired applications.

In this context, many asymmetric organic D- π -A systems have been synthesised.^[2] Nonlinearity/molecular structure relationships have emerged: the first hyperpolarisability and, hence, the second order NLO response is related to an electronic intramolecular charge transfer (ICT) excitation

between the ground and excited states of the molecule. The donor and acceptor strengths of the chromophores, and the extent of conjugation between them, are important factors in determining this response.^[1,3]

Tetrathiafulvalene (TTF) is a famous π -electron donor in the field of organic metals;^[4] one representative derivative is TTF-TCNQ (TCNQ = 7,7,8,8-tetracyano-*p*-quinodimethane),^[5] in which the delocalised electrons responsible for conduction originate from intermolecular charge transfer from TTF to the acceptor species. It is remarkable, therefore, that TTF has only recently been studied as a donor moiety in intramolecular charge transfer systems.^[6] This has been partly due to the synthetic challenge of obtaining unsymmetrically functionalised TTF derivatives. The recent efficient synthesis of TTF^[7] and the development of lithiation/electrophilic substitution methodology^[8] have overcome these problems.

The first NLO data for a TTF derivative were briefly reported recently by Andreu et al.^[9] Measurements on compound **1** in dioxane, using the EFISH technique at 1.38 μm , gave a $\mu\beta$ value of $85 \pm 5 \cdot 10^{-48}$, with $\mu = 4.8$ D and $\beta = 18 \cdot 10^{-30}$ esu. Since then, other stronger electron acceptor units have been attached covalently to the TTF fragment through different conjugated bridges,^[10] and values as high as $\mu\beta = 1350 \cdot 10^{-48}$ esu (1.907 μm , CH_2Cl_2) have recently been reported.^[11] These TTF- π -A systems (**2–4**) show the presence of an intramolecular charge transfer (ICT) band from the HOMO, which is localised on the TTF unit, to the LUMO, which spreads over the acceptor moiety. Interestingly, although the wavelength of the CT band decreases with increasing spacer conjugation length, the $\mu\beta$ values increase. To interpret these findings, it is of interest to study novel TTF- π -A systems endowed with moderate electron acceptor units. Therefore, we now report our studies on the synthesis, ICT and NLO properties of new TTF- π -A sys-

^[a] Department of Chemistry, University of Durham, South Road, Durham DH1 3LE, UK
Fax: (internat.) +44–191/384-4737
E-mail: m.r.bryce@durham.ac.uk

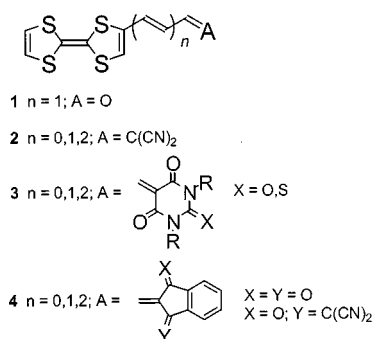
^[b] Laboratoire de Photonique Quantique et Moléculaire, Ecole Normale Supérieure
61, Avenue du Président Wilson, 94235 Cachan, France

^[c] Departamento de Química Orgánica, Facultad de Química, Universidad Complutense,
28040 Madrid, Spain

^[d] Departamento de Química Orgánica, ICMA, Universidad de Zaragoza-CSIC,
50009, Zaragoza, Spain

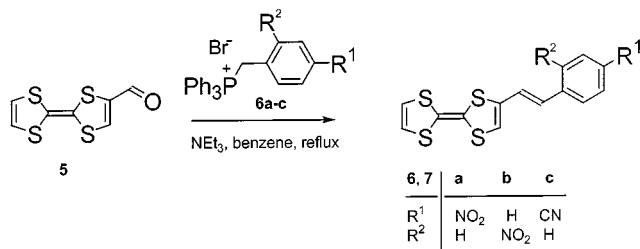
^[e] Departamento de Física de la Materia Condensada, ICMA, Universidad de Zaragoza-CSIC,
50009, Zaragoza, Spain

tems, in which electron-deficient aromatic groups act as the electron acceptor moieties.



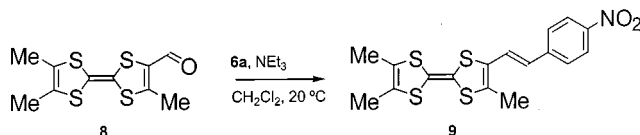
Results and Discussion

The synthesis of TTF- π -A derivatives **7a–c** was achieved by treatment of TTF-4-carboxaldehyde **5**^[12] with the Wittig reagents **6a–c** in the presence of triethylamine (Scheme 1). The products **7a–c** were formed as mixtures of (*E*) and (*Z*) isomers when the reaction was conducted at room temperature (¹H NMR evidence). Refluxing the product mixtures in benzene, however, gave the pure (*E*) isomers, which were isolated in 67–80% yields.



Scheme 1. Synthesis of compounds **7a–c**

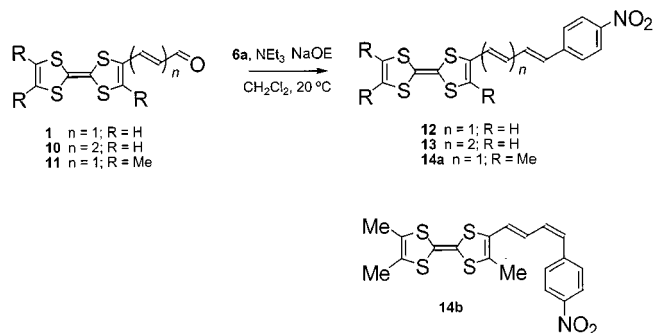
To explore the effect of increasing donor ability in the TTF unit, trimethyl-TTF derivative **8**^[13] was employed in a similar reaction with the ylide generated from **6a**, affording compound **9** in 62% yield (Scheme 2). Like previous trimethyl-TTF derivatives,^[13] compound **9** decomposed on silica gel; purification was, therefore, performed on neutral alumina with acid-free solvents.



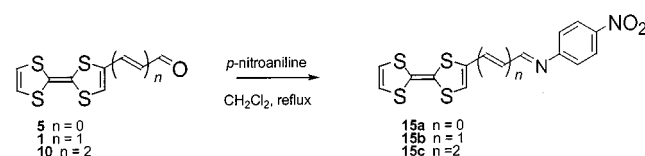
Scheme 2. Synthesis of compound **9**

To extend the length of the conjugated link between the D and A units, compounds **1**,^[12] **10**,^[14] and **11**^[13] were similarly converted into compounds **12**, **13**, and **14a/14b**, in 87, 52, and 29% yields, respectively (Scheme 3). In this series, compound **14b** is the only example of a pure (*Z*) alkene product being isolated. Imine analogues **15a–c** were prepared in moderate yields (42–56%) by treatment of the respective formyltetrafulvalene (**5**, **1**, and **10**, respectively)

with *p*-nitroaniline in dichloromethane (Scheme 4). Compounds **15a–c** undergo hydrolysis of the imino group during isolation on silica gel, resulting to some extent in the aldehyde and *p*-nitroaniline. This hydrolysis became more significant with increasing numbers of vinyl groups in the π -conjugated spacer, thus complicating the isolation and purification of compound **15b** and **15c**.



Scheme 3. Synthesis of compounds **12**, **13**, **14a**, and **14b**



Scheme 4. Synthesis of compounds **15a–c**

The structures of the new compounds were established by analytical and spectroscopic data. The ¹H NMR spectra of the TTF- π -acceptor molecules showed, in addition to the TTF protons observed as singlets at δ ca. 7.0 and 6.7, the aromatic protons as two doublets (AA'XX' system) at δ ca. 8.2 and 7.7 (*J* ca. 9 Hz). The vinyl protons (δ ca. 7.5–6.2) of the bridge were observed with different multiplicities, depending upon their position on the spacer chain. The coupling constants observed (*J* ca. 15 Hz) clearly indicate the all-*E* configuration (except **14b**, *J* = 9 Hz).

Cyclic voltammetric data for the new TTF derivatives **7a–c** showed small positive shifts, compared to unsubstituted TTF measured under the same conditions (Table 1), consistent with a slight increase in oxidation potential due to the conjugated aryl group. However, this was not the case when conjugation was extended further, as demonstrated by derivative **12**, for which the redox potentials were the same as TTF, within experimental error (± 10 mV). Trimethyl-TTF exhibits a stronger electron-donor character than the parent TTF, due to the presence of the three methyl groups.^[13] It is striking that trimethyl-TTF derivatives **9** and **14a** are considerably harder to oxidise relative to trimethyl-TTF ($\Delta E_1^{1/2} = 70$ –80 mV, $\Delta E_2^{1/2} = 40$ –50 mV) than compound **7a** is relative to TTF ($\Delta E_1^{1/2} = 20$ mV, $\Delta E_2^{1/2} = 0$ mV). This finding suggests that there is an increased degree of ICT in compounds **9** and **14a**. (A similar trend with smaller ΔE is seen for **14b**.)

Table 1. UV/Vis spectrophotometric and cyclic voltammetric data

Compound	$\lambda_{\text{max}}/\text{nm}$ ($\epsilon/\text{mol}^{-1}\text{Lcm}^{-1}$) ^[a]	$E_1^{1/2}/\text{V}^{[b]}$	$E_2^{1/2}/\text{V}^{[b]}$
7a	499 (3500)	0.45	0.77
7b	467 (4600)	0.45	0.81
7c	457 (3700)	0.45	0.81
9	516 (7500)	0.37	0.74
12	501 (4700)	0.42	0.78
13	506 (10200)	0.41	0.75
14a	513 (11800)	0.36	0.73
14b	499 (5400)	0.35	0.71
15a	522 ^[c]	— ^[c]	— ^[c]
TTF	—	0.43	0.77
TriMe-TTF	—	0.29	0.69

^[a] Data obtained in CH_2Cl_2 at 20 °C. — ^[b] Conditions are given in the Experimental Section. — ^[c] Not determined due to extensive decomposition.

The lowest energy absorption bands in the electronic spectra are given in Table 1. It is evident that, within the series of compounds **7a–c**, the $p\text{-NO}_2\text{-C}_6\text{H}_4$ group acts as the strongest acceptor, giving rise to the lowest energy ICT band. Increasing the donor strength of the TTF moiety by trimethyl substitution (compound **9**) predictably shifts the ICT band to lower energy (cf. compounds **7a** and **9**). It is notable that the ICT band for **12** and **13** remains nearly unaltered in comparison to **7a**. This behaviour is intermediate between that of compounds **2–4**^[10] and that observed for aldehydes **5**, **1**, and **10** (495 nm, 510 nm and 517 nm in CHCl_3 , respectively). A comparison of **14a** and **14b** shows that the (*E,E*) structure of the former facilitates the ICT process: the lowest energy absorption for **14b** is blue-shifted by 14 nm and the extinction coefficient is halved, relative to **14a**.

Negative solvatochromism was observed for the compounds **7a**, **9**, and **14a** (Table 2). However, this trend is not followed in dipolar aprotic solvents (DMSO and HCONH_2).

Table 2. The maxima of ICT bands of compounds **7b**, **9**, **14a** in different solvents

Solvent	ϵ ^[a]	7b	9 $\lambda_{\text{ICT}}/\text{nm}$	14a
<i>n</i> -Heptane	1.9	499	520	526
Toluene	2.4	507	523	
THF	7.4	501	509	
CH_2Cl_2	9.1	501	518	513
Acetone	20.7	492	497	
MeOH	32.6		498	490
MeCN	37.5	486	491	487
DMSO	48.9	507	510	
HCONH_2	111.5		515	

^[a] Relative permittivity: data from I. A. Koppel and V. A. Palm, in *Advances in Linear Free Energy Relationships*, (Eds.: N. B. Chapman and J. Shorter), Plenum, London, **1972**, ch. 5, p. 203; V. A. Palm, *Fundamentals of Quantitative Theory of Organic Reactions*, Khimiya, Leningrad, **1977**, p. 109 (in Russian).

The NLO properties were determined using the EFISH technique,^[15] performed in CH_2Cl_2 and CHCl_3 solution at 1.907 nm (the low solubility of compound **7c** in CH_2Cl_2

prevented an accurate measurement of its $\mu\beta$ value). The data are presented in Table 3. From experimental β values it is possible to infer “static” $\beta(0)$ values using a two-level dispersion model:^[15,16]

$$\beta = \frac{3\hbar^2 e^2}{2mW^3} \frac{W^4}{(W^2 - \hbar^2\omega^2)(W^2 - 4\hbar^2\omega^2)} f\Delta\mu = \frac{W^4}{(W^2 - \hbar^2\omega^2)(W^2 - 4\hbar^2\omega^2)} \beta(0)$$

where

$$\beta(0) = \beta_0 = \frac{3\hbar^2 e^2}{2m} \frac{f\Delta\mu}{W^3}$$

Here, $\hbar\omega$ is the energy of the excitation light, W is the energy of the charge transfer electronic transition, f the corresponding oscillator strength, $\Delta\mu = \mu_1 - \mu$ (where μ_1 is the dipole moment of the first excited state).

All the compounds studied exhibit moderate second order NLO properties (in comparison, the relevant application parameter is $\mu\beta(0)$, the standard value for the “classical” NLO dye DR1 is ca. $600 \cdot 10^{-48}$ esu). The $\mu\beta(0)$ values increase with increasing polyene bridge length. Thus, in the series **7a**, **12**, **13**, enhanced hyperpolarisability was obtained for compound **13**, bearing three vinyl units. It is interesting to note that compound **9**, containing the trimethyl-TTF moiety, shows a similar NLO response to **13** in spite of the shorter conjugated bridge in **9**. This finding suggests that trimethyl-TTF is a suitable donor for further NLO studies.

The $\mu\beta(0)$ values of the 4-nitrophenyl derivatives are higher than those of the corresponding aldehydes, which are included in Table 3 for comparison. This can be attributed to the stronger electron-withdrawing effect of the aryl substituent, and/or the longer linking group.

Table 3. Nonlinear optical data

Compound	$\mu\beta$ (10^{-48} esu) ^[a]	$\mu\beta(0)$ (10^{-48} esu) ^[a]
7a	225 ^[b]	150
9	370 ^[b]	240
12	270 ^[b]	180
13	315 ^[b]	210
15a	95 ^[b]	62
5	50 ^[c]	33
1	70 ^[c]	46
10	130 ^[c]	80

^[a] Estimated errors $< \pm 10\%$. — ^[b] Measured in CH_2Cl_2 at $\lambda = 1.907 \mu\text{m}$. — ^[c] Measured in CHCl_3 at $\lambda = 1.907 \mu\text{m}$.

The $\mu\beta(0)$ value determined for compound **15a**, endowed with an imino group as spacer, was notably lower than that obtained for the vinyl analogue **7a**; therefore, considering the low stability of these compounds, we did not pursue further measurements on imino derivatives.

The nonlinear optical responses of compounds **7a**, **7c**, **11**, **13**, and **15a** were also calculated by means of quantum chemical methods. Theoretical calculations were first performed using the semiempirical PM3 Hamiltonian^[17] since this method usually provides good qualitative and quantitative agreement with the experimentally measured NLO properties of TTF-derived chromophores at a low computational cost.^[18] Geometry optimisations considered the two possible conformations (**A** and **B** in Figure 1) of the single

bond linking the TTF moiety to the ethylenic spacer and resulted in planar structures. While the results suggest that conformer **B** is more stable than **A** in all the compounds studied, the small differences in the heats of formation calculated for these conformers, ranging from 0.92 to 1.88 kcal/mol (Table 4), indicate that both **A** and **B** should make a significant contribution to the experimentally measured second order polarisability, and hence we have calculated the NLO properties using the 'Finite Field' approach on these two geometries. The results of these calculations are presented in Table 4. It can be seen that semiempirical calculations can predict trends in the $\mu\beta$ values of these compounds while the absolute values are clearly overestimated. Quite surprisingly, the values calculated using conformations **A** and **B** are nearly identical, suggesting a small effect from conformation on the overall NLO response. Substitution of NO_2 by a CN group causes a decrease in both the dipole moment and the hyperpolarizability on passing from **7a** to **7c** and the imino compound **15a** is erroneously predicted to display behaviour similar to that of its ethylenic analogue **7a**. It is also noteworthy that the calculated dipole moment remains nearly unaltered on passing from compound **7a** to **12** and **13**. The change in the dipole moment expected from the charge separation caused by the increased length of the ethylenic bridge is countered by a decrease in the total charge supported by the donor and acceptor moieties and the enhanced $\mu\beta$ value should be solely due to an increase in the hyperpolarisability.

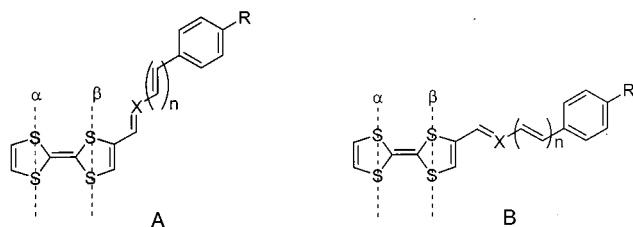


Figure 1. Proposed conformations of the compounds studied

In the search for a better agreement between theoretical and experimental values, calculations were also performed using ab initio methods. Geometries were optimised within the Restricted Hartree–Fock (RHF) formalism, using the Pople polarised, split valence, 6-31G* basis set,^[19] and the results in this case are different from those of PM3 calculations. Thus, conformation **A** is more stable than **B** by 1.76–2.64 kcal/mol (Table 5) and the optimised geometries

are not planar. The TTF moiety is folded along the S–S axes (α and β in Figure 1) as a consequence of the well known flexibility of TTF^[20] and in good agreement with theoretical calculations performed on other substituted TTFs.^[21] The calculated folding angles are 173.8–174.6° for α and 168.6–171.2° for β . Furthermore, the aromatic ring is rotated out of the plane defined by the ethylenic bridge, with a dihedral angle that ranges from 16.1 to 22.3°. An example of these optimised geometries is shown in Figure 2.

Ab initio hyperpolarisabilities were calculated using the CPHF (Coupled Perturbed Hartree–Fock) approach (Table 5). In contrast with PM3 results, the calculated hyperpolarisabilities differ depending on the conformation and the NLO response calculated for conformer **A** is always larger than that of **B**. The trends in hyperpolarisabilities calculated for these compounds are similar to those derived from PM3 calculations; however, ab initio methods yield a better quantitative agreement with the experimental values. Ab initio calculations of the dipole moments of compounds **7a**, **12**, and **13** also indicate that this property does not change on increasing the chain length, in agreement with PM3 results.

The topologies of the HOMO and LUMO were studied using the Density Functional Theory (DFT) with the aid of the B3LYP functional^[22] and the 6-31G* basis set, the choice of this functional set being due to its satisfactory calculation of the energy of orbitals.^[23]

The topologies of HOMO and LUMO (Figure 3) resemble those calculated for other TTF-derived chromophores;^[10] thus, the HOMO is mainly located on the TTF group and has the same topology as derived for the HOMO of unsubstituted TTF,^[24] while the LUMO is distributed over the acceptor moiety and shows the quinoid structure of the benzene ring in the excited state. The different locations of these orbitals indicate the charge transfer character of the HOMO–LUMO transition and show the HOMO–LUMO overlap necessary for obtaining large NLO responses.^[2c]

There is also a reasonable agreement between the experimental charge transfer absorption band and the calculated HOMO–LUMO gap. Thus, the experimental values for **7a**, **7c**, **12**, **13**, and **15a** are 2.48, 2.71, 2.47, 2.45, and 2.38 eV, and the calculated HOMO–LUMO gaps are 2.45, 2.81, 2.34, 2.27, and 2.25 eV, respectively.

Compound **9** is the only one in the present series for which X-ray quality crystals were obtained.^[25] It crystallises

Table 4. Results of FF-PM3 calculations

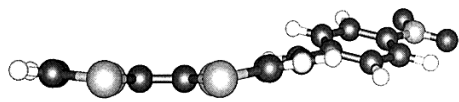
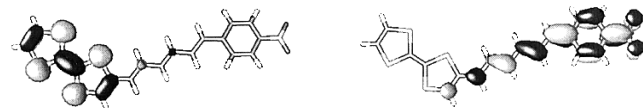
Compound	$\Delta H_f^{[a]}$	Conformer A $\mu^{[b]}$	$\mu\beta(0)^{[c]}$	$\Delta H_f^{[a]}$	Conformer B $\mu^{[b]}$	$\mu\beta(0)^{[c]}$	$\Delta H_{fB} - \Delta H_{fA}^{[a]}$
7a	104.30	5.93	207	103.38	5.91	203	−0.92
7c	148.14	3.64	69	147.18	3.61	67	−0.96
12	117.97	5.93	267	117.00	5.95	265	−0.97
13	131.72	5.95	319	130.75	5.98	315	−0.97
15a	113.58	5.58	199	111.70	5.94	213	−1.88

^[a] In kcal/mol. — ^[b] Debye. — ^[c] In ($\times 10^{-48}$ esu).

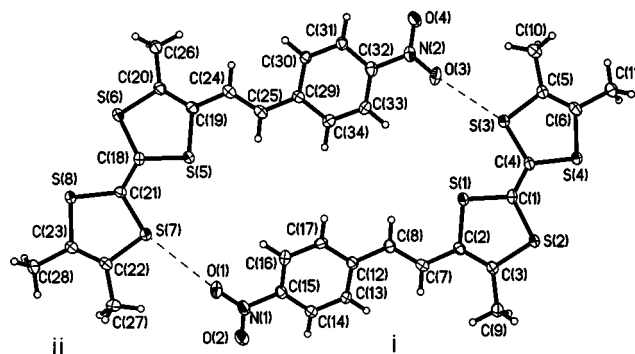
Table 5. Results of CPHF/6-31G**/HF/6-31G* calculations

Compound	$E^{[a]}$	Conformer A $\mu^{[b]}$	$\mu\beta(0)^{[c]}$	$E^{[a]}$	Conformer B $\mu^{[b]}$	$\mu\beta(0)^{[c]}$	$E_B - E_A^{[d]}$
7a	−2329.4200	5.80	137	−2329.4172	5.36	77	1.76
7c	−2217.6836	5.28	84	−2217.6808	4.86	40	1.76
12	−2406.3095	5.85	203	−2406.3065	5.43	123	1.88
13	−2483.1987	5.94	267	−2483.1958	5.47	168	1.82
15a	−2345.4175	6.48	113	−2345.4133	6.71	100	2.64

[a] In Hartree. — [b] Debye. — [c] In ($\times 10^{-48}$ esu). — [d] In kcal/mol.

Figure 2. Optimised geometry (HF/6-31G*) of compound **7a**Figure 3. Topologies (B3LYP/6-31G*) of the HOMO (left) and LUMO (right) of compound **13**

in the centrosymmetric space group $P\bar{1}$; hence no NLO properties were to be expected in the solid state. However, the structure gives ample evidence of ICT and also shows some interesting intermolecular interactions. The asymmetric unit (Figure 4) comprises two molecules (*i* and *ii*) with slightly different conformations but essentially coincident bond lengths. In molecule *i*, the TTF moiety is folded along the S(1)⋯S(2) vector ($\beta = 166^\circ$), the second dithiole ring remaining planar. In molecule *ii*, the entire TTF moiety is practically planar. In both molecules the torsion angles between the TTF and the olefinic bond, or between the benzene ring and the nitro group, are practically nil. The twist between the benzene ring and the ethylenic spacer — i.e., around the C(8)–C(12) and C(25)–C(29) bonds — is 19° and 9° , respectively. Thus, the observed conformations are qualitatively similar to the predicted ones, but more planarised. These conformations are favourable for an ICT interaction along the C(1)S(2)C(3)C(2)C(7)C(8)C(12) and C(18)S(6)C(20)C(19)C(24)C(25)C(29) chains, which manifests itself in the shortening of the C–C and C–S bonds and lengthening of the C=C bonds. The average carbon-carbon bond alternation^[26] in **9**, as compared to the fully π -localised structure, equals 0.03 \AA (6 e.s.d), while the shift from the localised to fully delocalised structure with all C–C bonds of 1.38 \AA implies bond alternation of ca. 0.08 \AA (Table 6). The dependence between bond alternation and the degree of ICT is known to be roughly linear;^[26b] hence the ICT in **9** can be estimated at ca. $0.4 e$.

Figure 4. Two independent molecules in the crystal of **9** (showing 50% thermal ellipsoids)Table 6. Bond lengths [\AA] in **9** vs. the standard values

	<i>i</i>		<i>ii</i>	Standard
S(1)–C(1)	1.768(4)	S(5)–C(18)	1.761(4)	1.762(1) ^[a]
S(1)–C(2)	1.769(4)	S(5)–C(19)	1.769(5)	1.767(1) ^[a]
S(2)–C(1)	1.756(5)	S(6)–C(18)	1.753(5)	1.762(1) ^[a]
S(2)–C(3)	1.751(4)	S(6)–C(20)	1.755(4)	1.767(1) ^[a]
C(2)–C(3)	1.361(6)	C(19)–C(20)	1.359(6)	1.342(2) ^[a]
C(2)–C(7)	1.441(6)	C(19)–C(24)	1.440(6)	1.478 ^[b]
C(7)–C(8)	1.349(6)	C(24)–C(25)	1.350(6)	1.312 ^[b]
C(8)–C(12)	1.457(6)	C(25)–C(29)	1.456(6)	1.488 ^[b]

[a] From the structure of tetramethyltetrathiafulvalene, ref.^[28] — [b] Unconjugated C(sp^2)–C(sp^2), C(sp^2)=C(sp^2) and C(sp^2)–C(aryl) bonds, ref.^[29]

Molecules *i* and *ii* are linked into a roughly planar pseudodimer (see Figure 4) through intermolecular contacts O(1)⋯S(7) $3.206(5) \text{ \AA}$ and O(3)⋯S(3) $2.926(5) \text{ \AA}$, which are shorter than the close van der Waals contact (3.25 \AA) and suggest weak donor-acceptor interactions.^[27a] The dimers are packed in layers, parallel to the crystallographic (1 0 $\bar{1}$) plane; this motif may be responsible for the flattening of the molecular conformation. Within the layer, dimers come into contact with each other through the TTF moieties (Figure 5), but the resulting S⋯S distances (3.95 – 4.00 \AA) are much longer than the normal van der Waals contact^[27b] of 3.60 \AA . Separations between mean planes of the layers are alternately 3.48 and 3.25 \AA . The former separation corresponds to an extensive overlap between molecule *ii* and its inversion equivalent; the nitro

group of one lies over a dithiole ring of the other, the olefin bond over the benzene ring. The latter separation is between laterally shifted layers with less effective overlap, such as between antiparallel nitrophenyl moieties of molecules *i* and *ii*, with the normal van der Waals C...C contacts (ca. 3.60 Å). Thus the molecules pack mainly in a head-to-tail (antiparallel) fashion, which minimises electrostatic repulsion – another proof of significant charge separation (ICT) in **9**. Such a motif naturally favours a centrosymmetric space group. At the same time, TTF moieties of (alternately) molecules *i* and *ii* form a stair-like stack, with the S...S contacts ranging from 3.52 to 3.64 Å; that is, equal to or slightly shorter than the standard van der Waals distance^[27b] of 3.61 Å. The latter synthon could be compatible with a chiral space group, which is a necessary precondition for solid state NLO properties, so there are grounds for moderate optimism concerning the possibility of obtaining such packing in this class of compounds.

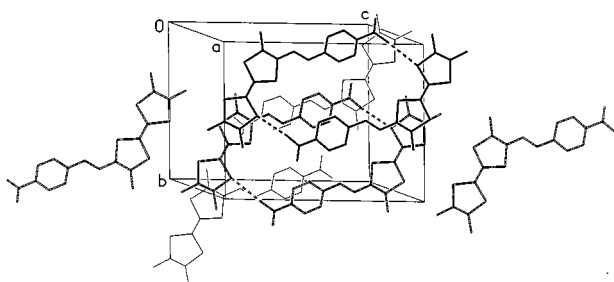


Figure 5. Crystal packing of **9**, projection on the (1 0 -1) plane

Conclusions

We have further developed the chemistry of functionalised TTF and trimethyl-TTF derivatives with the attachment of electron-deficient benzene acceptor groups through ethylenic bridges. These compounds display a broad ICT in their solution UV/Vis spectra. Regarding their nonlinear optical properties, the introduction of methyl substituents on the TTF core results in an increase in the NLO response. Moreover, the $\mu\beta(0)$ enhancement observed on increasing the length of the conjugated spacer does not result in a marked bathochromic shift, as is the case in most ICT systems. These results should encourage further studies on new TTF- π -A derivatives, with the aim of utilising the electron donor properties of the TTF system to produce new materials with interesting ICT and NLO properties.

Experimental Section

Column chromatography was performed on Merck silica gel (70–230 mesh), unless otherwise stated, and solvents were distilled prior to use. All reagents were of commercial quality and used as supplied unless otherwise stated; solvents were dried where necessary using standard procedures. – ¹H NMR spectra were obtained

on a Bruker AC 250 spectrometer operating at 250.134 MHz; coupling constants are quoted in Hz. ¹³C NMR spectra were obtained on a Varian 400 spectrometer operating at 100.581 MHz. – Mass spectra were recorded on a VG7070E spectrometer operating at 70 eV. – IR spectra were recorded on a Perkin–Elmer 1615 FTIR spectrometer operated from a Grams Analyst 1600. – UV/Vis absorption spectra were recorded with a Hitachi U-3400-UV/Vis-NIR spectrophotometer. – Melting points were obtained on a Kofler hot-stage microscope apparatus and are uncorrected. – Cyclic voltammetric data were obtained on a BAS 50 W electrochemical analyser (1.10^{−4} M solution of donor in acetonitrile under argon at 20 °C, 1.10^{−1} M Bu₄NClO₄ supporting electrolyte, platinum button working electrode and platinum wire counter electrode, Ag/AgCl reference electrode, 20 °C, scan rate 100 mV s^{−1}; Fc/Fc⁺ couple shows +0.43 V under these conditions). – EFISH measurements were taken with a nonlinear optics spectrometer from SOPRA. The fundamental light at 1.907 μm was the first Stokes peak of a hydrogen Raman cell pumped by the 1.064 μm light from a Q-switched Nd:YAG laser (Quintel YG 781, 10 pps, 8 ns, pulse). That light was passed through a linear polariser and focused on the EFISH cell. The polarising dc voltage (parallel to the light polarisation) used in this cell was 6 kV. The output light from the cell was passed through an interference filter to select the second harmonic light (0.954 μm) which was finally detected with a R642 photomultiplier from Hamamatsu. Static $\beta(0)$ values were deduced from the experimental values using a two-level dispersion model. – Molecular orbital calculations were performed on Intel Pentium Pro-based and Pentium III-based computers running under Windows NT 4.0. Semiempirical calculations used the MOPAC 6.0 package program^[30] while HF and DFT calculations were performed with the Gaussian 98w program.^[31]

X-ray Crystallography: A single crystal (0.04 × 0.11 × 0.22 mm) of **9**, suitable for X-ray diffraction study, was grown from MeCN. The experiment was performed at *T* = 120 K on a SMART 3-circle diffractometer with a 1 K CCD area detector, using Mo-*K*_α radiation (λ = 0.71073 Å). The structure was solved by direct methods and refined by full-matrix, least-squares against *F*² of all data, using SHELXTL programs.^[32] *Crystal data:* C₁₇H₁₅NO₂S₄, *M*_w 393.54, triclinic, space group *P* $\bar{1}$ (No. 2), *a* = 8.093(1), *b* = 12.495(2), *c* = 17.668(3) Å, α = 88.15(1), β = 81.38(1), γ = 78.79(1)°, *U* = 1732.7(5) Å³, *Z* = 4, μ = 0.56 mm^{−1}, 12669 reflections (2θ ≤ 55°), 7843 unique, *R*_{int} = 0.068, 445 refined parameters, *R* = 0.062 [4699 data with *F*² ≥ σ(*F*²)], *wR*(*F*²) = 0.168. Full structural data (excluding structure factors) have been deposited at the Cambridge Crystallographic Data Centre as supplementary publication no CCDC-145576.

General Procedure for Compounds 7a–c: Triethylamine (3.0 equiv.) was added to a stirred suspension of the corresponding Wittig reagent **6a–c** (3.0 equiv.) in dry benzene. This was followed by 4-formyltetrathiafulvalene **5**^[10] (1.0 equiv.), in one portion under a positive flow of argon. The resulting dark solution was heated under reflux for 4 h. The solution was allowed to cool and the solvent removed in vacuo to yield a black residue which was purified by column chromatography, yielding compounds **7a–c**.

2-(4-Nitrophenyl)-1-(tetrathiafulvalen-4-yl)ethene (7a): Reagent **6a** (3.71 g, 7.76 mmol), benzene (50 mL), triethylamine (1.08 mL, 7.76 mmol), and **5** (0.6 g, 2.59 mmol), with dichloromethane/hexane (5:3 v/v) as eluent, yielded compound **7a** as a purple solid (0.73 g, 80%). M.p. 237–238 °C. – C₁₄H₉NO₂S₄ (351.5): calcd. C 47.86, H 2.56, N 3.96; found C 47.85, H 2.33, N 3.72. – ¹H NMR (CDCl₃): δ = 8.18 (d, *J* = 9 Hz, 2 H), 7.56 (d, *J* = 9 Hz, 2 H), 7.07 (d, *J* = 15 Hz, 1 H), 6.72 (d, *J* = 15 Hz, 1 H), 6.61 (s, 1 H),

6.38 (s, 2 H). – ^{13}C NMR (CDCl_3): 146.2, 143.1, 134.6, 131.7, 131.5, 128.5, 127.2, 124.9, 124.5, 123.9, 120.0, 113.0. – MS (EI): m/z (%) 351 (100) [M^+]. – IR (KBr): $\tilde{\nu}$ = 1567, 1522, 1290, 1106, 975, 545 cm^{-1} . – UV (CH_2Cl_2): λ_{max} 292, 338, 499 nm.

2-(2-Nitrophenyl)-1-(tetrathiafulvalen-4-yl)ethene (7b): Reagent **6b** (2.06 g, 4.31 mmol), benzene (50 mL), triethylamine (0.60 mL, 4.3 mmol), and **5** (0.10 g, 0.43 mmol), with dichloromethane/hexane (1:1 v/v) as eluent, yielded compound **7b** as a black solid (0.10 g, 67%). M.p. 159–160 °C. – $\text{C}_{14}\text{H}_9\text{NO}_2\text{S}_4$ (351.5): calcd. C 47.86, H 2.56, N 3.98; found C 47.42, H 2.58, N 3.76. – ^1H NMR [$(\text{CD}_3)_2\text{CO}$]: δ = 8.01 (d, J = 8 Hz, 1 H), 7.92 (d, J = 8 Hz, 1 H), 7.72 (t, J = 8 Hz, 1 H), 7.56 (t, J = 8 Hz, 1 H), 7.28 (d, J = 16 Hz, 1 H), 6.98 (s, 1 H), 6.85 (d, J = 16 Hz, 1 H), 6.67 (s, 2 H). – MS (EI): m/z (%) 351 (100) [M^+]. – IR (KBr): $\tilde{\nu}$ = 1513, 1471, 1346, 1331, 1273, 1253 cm^{-1} . – UV (CH_2Cl_2): λ_{max} 299, 320sh, 467 nm.

2-(4-Cyanophenyl)-1-(tetrathiafulvalen-4-yl)ethene (7c): Reagent **6c** (1.78 g, 4.31 mmol), benzene (50 mL), triethylamine (0.60 mL, 4.3 mmol), and **5** (0.10 g, 0.43 mmol), with dichloromethane as eluent, yielded compound **7c** as a deep purple solid (0.10 g, 70%). M.p. 121–122 °C. – $\text{C}_{15}\text{H}_9\text{NS}_4$ (331.5): calcd. C 54.35, H 2.74, N 4.23; found C 54.56, H 2.77, N 4.00. – ^1H NMR (CDCl_3): δ = 7.76 (s, 4 H), 7.41 (d, J = 13 Hz, 1 H), 6.97 (s, 1 H), 6.79 (s, 2 H), 6.52 (d, J = 13 Hz, 1 H). – MS (DCI): m/z (%) 332 (100) [$\text{M}^+ + 1$]. – IR (KBr): $\tilde{\nu}$ = 1654, 1548, 1468, 1245, 1095, 995 cm^{-1} . – UV (CH_2Cl_2): λ_{max} 277, 457 nm.

2-(4-Nitrophenyl)-1-(4',5,5'-trimethyltetrathiafulvalen-4-yl)ethene (9): This compound was prepared according to the general procedure outlined for **7a–c**. Reagent **6a** (0.55 g, 1.14 mmol), benzene (50 mL), triethylamine (1 mL, excess), and **8** (0.1 g, 0.38 mmol) yielded compound **6** as a black solid (0.85 g, 75%) after chromatography on neutral alumina, eluent dichloromethane. M.p. > 250 °C. – $\text{C}_{17}\text{H}_{15}\text{NO}_2\text{S}_4$ (393.6): calcd. C 69.86, H 3.81, N 3.56; found C 69.88, H 4.01, N 3.45. – ^1H NMR (CDCl_3): δ = 8.12 (d, J = 8 Hz, 2 H), 7.68 (d, J = 8 Hz, 2 H), 6.99 (d, J = 15 Hz, 1 H), 6.75 (d, J = 15 Hz, 1 H), 2.30 (s, 3 H), 2.18 (s, 6 H). – MS (DCI): m/z (%) 394 (100) [$\text{M}^+ + 1$]. – IR (KBr): $\tilde{\nu}$ = 1543, 1520, 1277, 1100, 938, 510 cm^{-1} . – UV (CH_2Cl_2): λ_{max} 345, 516 nm.

(1E,3E)-4-(4-Nitrobenzyl)-1-(tetrathiafulvalen-4-yl)buta-1,3-diene (12): Triethylamine (3 mL, excess) was added to a solution of reagent **6a** (1.70 g, 3.55 mmol) in dichloromethane (50 mL), followed dropwise by compound **1** (0.10 g, 1.18 mmol), as a solution in dichloromethane (50 mL). The mixture was stirred at 20 °C for 48 h, after which time the solvent was removed in vacuo and the residue purified by silica gel chromatography (eluent dichloromethane/hexane 1:1 v/v) followed by recrystallisation from dichloromethane/hexane (1:10 v/v) to yield compound **12** (0.10 g, 87%). M.p. 224–225 °C. – $\text{C}_{16}\text{H}_{11}\text{NO}_2\text{S}_4$ (337.5): calcd. C 52.71, H 2.91, N 3.71; found C 52.68, H 3.11, N 3.79. – ^1H NMR (CDCl_3): δ = 8.23 (d, J = 8 Hz, 2 H), 8.01 (d, J = 8 Hz, 2 H), 7.65 (d, J = 15 Hz, 1 H), 7.34–7.32 (m, 2 H), 6.99 (s, 1 H), 6.96 (d, J = 15 Hz, 1 H), 6.40 (s, 2 H). – MS (DCI): m/z (%) 378 (100) [$\text{M}^+ + 1$]. – IR (KBr): $\tilde{\nu}$ = 1657, 1644, 1590, 1499, 1488, 1205 cm^{-1} . – UV (CH_2Cl_2): λ_{max} 298, 362, 501 nm.

(1E,3E,5E)-6-(4-Nitrobenzyl)-1-(tetrathiafulvalen-4-yl)hexa-1,3,5-triene (13): Under argon atmosphere, a solution of sodium ethoxide prepared from sodium (50 mg) and dry ethanol (6 mL) was added to a solution of 5-(tetrathiafulvalenyl)penta-2,4-dien-1-yl^[14] (**10**) (280 mg, 1.0 mmol) and **6a** (480 mg, 1.0 mmol) in dry ethanol (15 mL). The reaction mixture was refluxed for 2 h and was then allowed to cool to room temperature. Water (15 mL) was added and the mixture was extracted several times with dichloromethane.

The combined organic layers were dried with magnesium sulfate, the solvent was removed under vacuum, and the crude product was chromatographed (eluent hexane/dichloromethane) to yield **13** (340 mg, 52%). M.p. 207–208 °C. – $\text{C}_{18}\text{H}_{13}\text{NO}_2\text{S}_4$ (403.6): calcd. C 53.60, H 3.25, N 3.47; found C 53.99, H 3.48, N 3.77. – ^1H NMR ($[\text{D}_6]\text{DMSO}$): δ 8.17 (d, J = 9.3 Hz, 2 H), 7.74 (d, J = 8.7 Hz, 2 H), 7.28 (m, 2 H), 6.94 (s, 1 H), 6.75, (m, 2 H), 6.70 (d, J = 14.4 Hz, 1 H), 6.63 (d, J = 11.7 Hz, 1 H), 6.22 (m, 2 H). – ^{13}C NMR ($[\text{D}_6]\text{DMSO}$): δ = 145.4, 143.5, 135.1, 134.5, 133.9, 133.5, 131.1, 130.1, 126.1, 124.9, 123.6, 121.1, 119.6, 115.1, 113.7, 112.2, 112.1. – MS (EI): m/z (%) = 403 (100) [M^+]. – IR (KBr): $\tilde{\nu}$ = 2921, 1584, 1505, 1340, 1259, 1107, 1002 cm^{-1} . – UV (CH_2Cl_2): λ_{max} 240, 324, 388, 506 nm.

(E,E)-6-(4-Nitrophenyl)-1-(4',5,5'-trimethyltetrathiafulvalen-4-yl)buta-1,3-diene (14a) and (E,Z)-6-(4-Nitrophenyl)-1-(4',5,5'-trimethyltetrathiafulvalen-4-yl)buta-1,3-diene (14b): Triethylamine (0.50 mL, excess) was added to a solution of reagent **6a** (300 mg, 0.628 mmol) in dry CH_2Cl_2 (12 mL), followed by aldehyde **11**^[13] (60 mg, 0.20 mmol) and the reaction mixture was stirred at 20 °C for 72 h. TLC monitoring showed the presence of two isomers, and so an attempt to isomerise the mixture to afford solely the *trans*,*trans* isomer was undertaken by refluxing the crude product in benzene (after removing CH_2Cl_2). No isomerisation was observed, however. The solvent was removed in vacuo and the residue was chromatographed on silica, eluting with chloroform/hexane mixture (3:2 v/v) basified with a few drops of triethylamine. The first, brown-violet fraction gave pure *trans*,*cis* isomer **14b** (9.5 mg). M.p. 194 °C. It was immediately followed by the second fraction, of similar colour, which gave a mixture of **14a** and **14b** in the ratio 4:1 (14.5 mg; total yield of **14a** and **14b** 29%). Recrystallisation from toluene (1 mL) yielded almost pure *trans*,*trans* isomer **14a** (9 mg). M.p. 236–239 °C (contaminated with 8% of *trans*,*cis*-impurity, as judged by ^1H NMR).

Compound 14a: $\text{C}_{19}\text{H}_{17}\text{NO}_2\text{S}_4$ (419.6) calcd. C 54.39, H 4.08, N 3.34; found C 54.75, H 4.33, N 3.19. – ^1H NMR [$(\text{CD}_3)_2\text{CO}$]: δ = 8.21 (d, J = 9 Hz, 2 H), 7.74 (d, J = 9 Hz, 2 H), 7.31 (dd, J = 10.5 and 15.5 Hz, 1 H), 6.92 (d, J = 15.5 Hz, 1 H), 6.89 (d, J = 15.0 Hz, 1 H), 6.33 (dd, J = 10.5 and 15.0 Hz, 1 H), 2.20 (s, 3 H), 1.98 (s, 6 H). – MS (EI): m/z (%) = 419 (100) [M^+]. – UV (CH_2Cl_2): λ_{max} 298, 369, 513.

Compound 14b: $\text{C}_{19}\text{H}_{17}\text{NO}_2\text{S}_4$ (419.6) calcd. C 54.39, H 4.08, N 3.34; found C 54.09, H 4.12, N 3.25. – ^1H NMR [$(\text{CD}_3)_2\text{CO}$]: δ = 8.30 (d, J = 9 Hz, 2 H), 7.67 (d, J = 9 Hz, 2 H), 6.93 (d, J = 14 Hz, 1 H), 6.52–6.68 (m, 3 H), 2.20 (s, 3 H), 1.96 (s, 6 H). – MS (EI): m/z (%) = 419 (30) [M^+]. – UV (CH_2Cl_2): λ_{max} 298, 335sh, 370sh, 499 nm.

General Procedure for Compounds 15a–c: *p*-Nitroaniline (1 mmol) was added to a stirred solution of the corresponding formyl-TTF derivative (**5**, **1**, **10**) (1 mmol) in dry dichloromethane (30 mL). The reaction mixture was allowed to reflux overnight under argon atmosphere in the presence of 4 Å molecular sieves. After the reaction mixture had been allowed to reach room temperature, it was filtered and the solvent was removed under vacuum to yield a solid that was purified by column chromatography (eluent hexane/diethyl ether).

4-Nitro-*N*-(tetrathiafulvalen-4-ylmethylene)aniline (15a): Following the general procedure above, **15a** was obtained in 56% yield. M.p. 173–175 °C (decomp.). – $\text{C}_{13}\text{H}_8\text{N}_2\text{O}_2\text{S}_4$ (352.5): calcd. C 44.32, H 2.27, N 7.95; found C 44.89, H 2.53, N 8.48. – ^1H NMR (CDCl_3): δ 8.25 (d, J = 9 Hz, 2 H), 8.15 (s, 1 H), 7.21 (d, J = 9 Hz, 2 H), 7.13 (s, 1 H), 6.36 (d, J = 6 Hz, 1 H), 6.34 (d, J = 6 Hz, 1 H). –

^{13}C NMR (CDCl_3): δ = 164.3, 155.2, 145.4, 144.9, 127.9, 127.7, 126.2, 126.0, 124.7, 124.2, 122.3, 110.4, 109.8. – MS (EI): m/z (%) = 352 (100) $[\text{M}^+]$. – IR (KBr): $\tilde{\nu}$ = 1600, 1565, 1535, 1515, 1335, 1165, 1115 cm^{-1} . – UV (CH_2Cl_2): λ_{max} 328, 522 nm.

4-Nitro-*N*-[3-(tetrathiafulvalen-4-yl)propenylidene]aniline (15b): Following the general procedure above, **15b** was obtained in 51% yield. M.p. 158–160 °C (decomp.). – $\text{C}_{15}\text{H}_{10}\text{N}_2\text{O}_2\text{S}_4$ (378.5): calcd. C 47.60, H 2.66, N 7.40; found C 47.84; H 2.99; N 7.19. – ^1H NMR (CDCl_3): δ 8.25, 8.09 (AA'XX', 4 H), 7.19 (d, J = 9 Hz, 1 H), 6.98 (d, J = 15 Hz, 1 H), 6.72 (s, 1 H), 6.38 (dd, J = 15 Hz, J' = 9 Hz, 1 H), 6.34 (s, 2 H). – ^{13}C NMR (CDCl_3): δ = 167.8, 154.9, 146.5, 144.4, 127.3, 127.1, 126.8, 126.5, 124.9, 124.5, 123.1, 121.9, 119.6, 112.7, 112.3. – MS (EI): m/z (%) = 378 (100) $[\text{M}^+]$. – IR (KBr): $\tilde{\nu}$ = 1600, 1575, 1510, 1345, 1150, 1110 cm^{-1} . – UV (CH_2Cl_2): λ_{max} 322, 514 nm.

4-Nitro-*N*-[5-(tetrathiafulvalen-4-yl)pentadienylidene]aniline (15c): Following the general procedure above, **15c** was obtained in 42% yield. M.p. 141–143 °C (decomp.). – $\text{C}_{17}\text{H}_{12}\text{N}_2\text{O}_2\text{S}_4$ (404.5): calcd. C 50.47, H 2.99, N 6.92; found C 50.77, H 3.32, N 7.12. – ^1H NMR (CDCl_3): δ 8.23, 8.11 (AA'XX', 4 H), 7.21 (d, J = 9 Hz, 1 H), 6.84 (d, J = 15 Hz, 1 H), 6.72 (s, 1 H), 6.64–6.52 (m, 2 H), 6.41 (dd, J = 15 Hz, J' = 9 Hz, 1 H), 6.34 (s, 2 H). – MS (EI): m/z (%) = 404 (100) $[\text{M}^+]$. – IR (KBr): $\tilde{\nu}$ = 1595, 1560, 1515, 1335, 1155, 1110 cm^{-1} . – UV (CH_2Cl_2): λ_{max} 239, 334, 502 nm.

Acknowledgments

We thank EPSRC for funding the work at Durham, and Zeneca for a CASE Award (to A. G.). J.A.K.H. thanks the EPSRC for a Senior Research Fellowship. The Spanish groups thank the DGICYT (Projects PB98-0818 and MAT99-1009-C02-02) for financial support.

- [1] [1a] *Nonlinear Optical Properties of Organic Molecules and Crystals* (Eds.: D. S. Chemla, J. Zyss) Academic Press, Boston, **1987**. – [1b] *Introduction to Nonlinear Optical Effects in Molecules and Polymers* (Eds.: P. N. Prasad, D. J. Williams), Wiley, New York, **1991**. – [1c] *Molecular Nonlinear Optics: Materials, Physics and Devices* (Ed.: J. Zyss) Academic Press, Boston, **1994**. – [1d] S. R. Marder, B. Kippelen, A. K.-Y. Jen, N. Peyghambarian, *Nature* **1997**, *388*, 845–851. – [1e] G. J. Ashwell, *J. Mater. Chem.* **1999**, *9*, 1991–2003.
- [2] [2a] T. Verbiest, S. Houbrechts, M. Kauranen, K. Clays, A. Persoons, *J. Mater. Chem.* **1997**, *7*, 2175–2189. – [2b] *Characterization Techniques and Tabulations for Organic Nonlinear Optical Materials*, (Eds.: M. G. Kuzyk, C. W. Dirk) Dekker **1998**. – [2c] D. R. Kanis, M. A. Ratner, T. J. Marks, *Chem. Rev.* **1994**, *94*, 195–242.
- [3] [3a] S. R. Marder, L.-T. Cheng, B. G. Tiemann, A. C. Friedli, M. Blanchard-Desce, J. W. Perry, J. Skindhøj, *Science* **1994**, *263*, 511–514. – [3b] L. T. Cheng, W. Tam, S. Marder, A. E. Stegman, G. Rikken, C. W. Spangler, *J. Phys. Chem.* **1991**, *95*, 10643–10652. – [3c] L. T. Cheng, W. Tam, S. H. Stevenson, G. R. Meredith, G. Rikken, S. R. Marder, *J. Phys. Chem.* **1991**, *95*, 10631–10643. – [3d] S. R. Marder, D. N. Beratan, L.-T. Cheng, *Science* **1991**, *252*, 103–106.
- [4] For initial references to TTF see: [4a] F. Wudl, G. M. Smith, E. J. Hufnagel, *J. Chem. Soc., Chem. Commun.* **1970**, 1453–1454. – [4b] S. Hünig, G. Kiesslich, H. Quast, D. Scheutzw, *Justus Liebigs Ann. Chem.* **1973**, 310–323. – For recent reviews see: [4c] G. Schukat, A. M. Richter, E. Fanghanel, *Sulfur Rep.* **1987**, *7*, 155–240. – [4d] G. C. Papavassiliou, A. Terzis, P. Delhaës, in: *Handbook of Conductive Molecules and Polymers*, Vol. 1, (Ed.: H. S. Nalwa) J. Wiley and Sons, Chichester **1997**, 152–227. – [4e] J. Yamada, H. Nishikawa, K. Kikuchi, *J. Mater. Chem.* **1999**, *9*, 617–628. – [4f] M. R. Bryce, *J. Mater. Chem.* **2000**, *10*, 589–598.
- [5] J. Ferraris, D. O. Cowan, V. V. Walatka, J. H. Perlstein, *J. Am. Chem. Soc.* **1973**, *95*, 948–949.
- [6] Review: M. R. Bryce, *Adv. Mater.* **1999**, *11*, 11–23.
- [7] A. J. Moore, M. R. Bryce, *Synthesis* **1997**, 407–409.
- [8] Review: J. Garin, *Adv. Heterocycl. Chem.* **1995**, *62*, 249–304.
- [9] R. Andreu, A. I. de Lucas, J. Garin, N. Martín, J. Orduna, L. Sánchez, C. Seoane, *Synth. Met.* **1997**, *86*, 1817–1818.
- [10] [10a] A. I. De Lucas, N. Martín, L. Sánchez, C. Seoane, R. Andreu, J. Garin, J. Orduna, *Tetrahedron* **1998**, *54*, 4655–4662. [10b] J. Garin, J. Orduna, J. Rupérez, R. Alcalá, B. Villacampa, C. Sánchez, N. Martín, J. L. Segura, M. González, *Tetrahedron Lett.* **1998**, *39*, 3577–3580.
- [11] M. González, N. Martín, J. L. Segura, C. Seoane, J. Garin, J. Orduna, R. Alcalá, C. Sánchez, B. Villacampa, *Tetrahedron Lett.* **1999**, *40*, 8599–8602.
- [12] J. Garin, J. Orduna, S. Uriel, A. J. Moore, M. R. Bryce, S. Wegener, D. S. Yufit, J. A. K. Howard, *Synthesis* **1994**, 489–493.
- [13] A. J. Moore, M. R. Bryce, A. S. Batsanov, J. C. Cole, J. A. K. Howard, *Synthesis* **1995**, 675–682.
- [14] M. González, N. Martín, J. L. Segura, J. Garin, J. Orduna, *Tetrahedron Lett.* **1998**, *39*, 3269–3272.
- [15] [15a] J. L. Oudar, *J. Chem. Phys.* **1977**, *67*, 446–457. – [15b] B. F. Levine, C. G. Bethea, *J. Chem. Phys.* **1975**, *63*, 2666–2682.
- [16] J. L. Oudar, D. S. Chemla, *J. Chem. Phys.* **1977**, *66*, 2664–2668.
- [17] [17a] J. J. P. Stewart, *J. Comput. Chem.* **1989**, *10*, 209–220. [17b] J. J. P. Stewart, *J. Comput. Chem.* **1989**, *10*, 221–264.
- [18] J. Garin, J. Orduna, R. Andreu, *Synth. Met.* **1999**, *102*, 1531–1532.
- [19] P. C. Hariharan, J. A. Pople, *Chem. Phys. Lett.* **1972**, *16*, 217–219.
- [20] R. Viruela, P. M. Viruela, R. Pou-Américo, E. Ortí, *Synth. Met.* **1999**, *103*, 1991–1992.
- [21] E. Demilrap, S. Dasgupta, W. A. Goddard III, *J. Am. Chem. Soc.* **1995**, *117*, 8154–8158. E. Demilrap, W. A. Goddard III, *J. Phys. Chem.* **1997**, *101*, 8128–8131.
- [22] A. D. Becke, *J. Chem. Phys.* **1993**, *98*, 5648–5652.
- [23] U. Saltzner, J. B. Lagowsky, P. G. Pickup, R. A. Poirier, *J. Comput. Chem.* **1997**, *15*, 1943–1953.
- [24] A. S. Batsanov, M. R. Bryce, J. N. Heaton, A. J. Moore, P. J. Skabara, J. A. K. Howard, E. Ortí, P. M. Viruela, R. Viruela, *J. Mater. Chem.* **1995**, *5*, 1689–1696.
- [25] For crystal structures of conjugated TTF- π -A molecules see: [25a] A. Aqad, A. Ellern, L. Shapiro, V. Khodorkovsky, *Tetrahedron Lett.* **2000**, *41*, 2983–2986. – [25b] R. Andreu, I. Malfant, P. G. Lacroix, P. Cassoux, *Eur. J. Org. Chem.* **2000**, 737–741.
- [26] [26a] S. R. Marder, J. W. Perry, B. G. Tiemann, C. B. Gorman, S. Gilmour, S. L. Biddle, G. Bourhill, *J. Am. Chem. Soc.* **1993**, *115*, 2524–2546. – [26b] J. C. Cole, J. M. Cole, G. H. Cross, M. Farsari, J. A. K. Howard, M. Szablewski, *Acta Crystallogr. Sect. B* **1997**, *53*, 812–821.
- [27] [27a] A. Kucsman, I. Kapovits, in: *Organic Sulfur Chemistry*, F. Bernardi, I. G. Csizmadia, A. Mangini eds. Elsevier: Amsterdam, 1985, p. 191–245. – [27b] R. S. Rowland, R. Taylor, *J. Chem. Phys.* **1996**, *100*, 7384–7391.
- [28] A. S. Batsanov, M. R. Bryce, A. Chesney, J. A. K. Howard, D. E. John, A. J. Moore, C. L. Wood, H. Gershtenman, J. Y. Becker, V. Y. Khodorkovsky, A. Ellern, J. Bernstein, I. F. Perepichka, V. Rotello, *J. Mater. Chem.* Manuscript in preparation.
- [29] F. H. Allen, O. Kennard, D. G. Watson, L. Brammer, A. G. Orpen, R. Taylor, *J. Chem. Soc., Perkin Trans. 2* **1987**, Supplement 1–19.
- [30] *MOPAC 6.0*: J. J. P. Stewart, QCPE, **1990**, *10*, 455.
- [31] *Gaussian 98W*, Revision A.7, M. J. Frisch, G. W. Trucks, H. B. Schlegel, G. E. Scuseria, M. A. Robb, J. R. Cheeseman, V. G. Zakrzewski, J. A. Montgomery, Jr., R. E. Stratmann, J. C. Burant, S. Dapprich, J. M. Millam, A. D. Daniels, K. N. Kudin, M. C. Strain, O. Farkas, J. Tomasi, V. Barone, M. Cossi, R. Cammi, B. Mennucci, C. Pomelli, C. Adamo, S. Clifford, J. Ochterski, G. A. Petersson, P. Y. Ayala, Q. Cui, K. Morokuma, D. K. Malick, A. D. Rabuck, K. Raghavachari, J. B. Foresman, J. Cioslowski, J. V. Ortiz, A. G. Baboul, B. B. Stefanov, G. Liu, A. Liashenko, P. Piskorz, I. Komaromi, R. Gomperts, R. L. Martin, D. J. Fox, T. Keith, M. A. Al-Laham, C. Y. Peng, A. Nanayakkara, C. Gonzalez, M. Challacombe, P. M. W. Gill, B.

Johnson, W. Chen, M. W. Wong, J. L. Andres, C. Gonzalez, M. Head-Gordon, E. S. Replogle, J. A. Pople, Gaussian, Inc., Pittsburgh PA, **1998**.

[32] *SHELXTL*, An integrated system for solving, refining and dis-

playing crystal structures from diffraction data, Ver. 5.10 (**1997**), Bruker Analytical X-ray Systems, Madison, WI, U.S.A.

Received October 9, 2000

[O00520]